Geophysical Research Letters

RESEARCH LETTER
10.1029/2023GL107399

Lagrangian Decomposition of the Atlantic Ocean Heat Transport at 26.5°N

Oliver J. Tooth[1], Nicholas P. Foukal[2], William E. Johns[3], Helen L. Johnson[1], and Chris Wilson[4]

[1]Department of Earth Sciences, University of Oxford, Oxford, UK, [2]Department of Physical Oceanography, Woods Hole Oceanographic Institution, Woods Hole, MA, USA, [3]Rosenstiel School of Marine, Atmospheric, and Earth Science, University of Miami, Miami, FL, USA, [4]National Oceanography Centre, Liverpool, UK

Key Points:

- Water parcels recirculating in the subtropical gyre account for 37% of the total heat transport at 26.5°N in an eddy-rich ocean hindcast
- The heat transport of the subtropical gyre is associated with shallow vertical overturning rather than the horizontal circulation at 26.5°N
- Both horizontal and vertical circulation cells are fundamental components of the Atlantic Meridional Overturning Circulation

Supporting Information:

Supporting Information may be found in the online version of this article.

Correspondence to:

O. J. Tooth,
oliver.tooth@seh.ox.ac.uk

Citation:

Tooth, O. J., Foukal, N. P., Johns, W. E., Johnson, H. L., & Wilson, C. (2024). Lagrangian decomposition of the Atlantic Ocean heat transport at 26.5°N. *Geophysical Research Letters*, *51*, e2023GL107399. https://doi.org/10.1029/2023GL107399

Received 19 NOV 2023
Accepted 4 JUL 2024

Author Contributions:

Conceptualization: Oliver J. Tooth, Nicholas P. Foukal, William E. Johns
Investigation: Oliver J. Tooth
Methodology: Oliver J. Tooth, Nicholas P. Foukal, William E. Johns, Chris Wilson
Resources: William E. Johns
Software: Oliver J. Tooth
Supervision: Helen L. Johnson, Chris Wilson
Visualization: Oliver J. Tooth, Nicholas P. Foukal
Writing – original draft: Oliver J. Tooth

Abstract The Atlantic Meridional Overturning Circulation (AMOC) plays a critical role in the global climate system through the redistribution of heat, freshwater and carbon. At 26.5°N, the meridional heat transport has traditionally been partitioned geometrically into vertical and horizontal circulation cells; however, attributing these components to the AMOC and Subtropical Gyre (STG) flow structures remains widely debated. Using water parcel trajectories evaluated within an eddy-rich ocean hindcast, we present the first Lagrangian decomposition of the meridional heat transport at 26.5°N. We find that water parcels recirculating within the STG account for 37% (0.36 PW) of the total heat transport across 26.5°N, more than twice that of the classical horizontal gyre component (15%). Our findings indicate that STG heat transport cannot be meaningfully distinguished from that of the basin-scale overturning since water parcels cooled within the gyre subsequently feed the northward, subsurface limb of the AMOC.

Plain Language Summary The Atlantic Meridional Overturning Circulation transports heat northward by converting warm, surface waters into cold waters returning at depth. In the subtropical North Atlantic, the heat transported by the overturning circulation has traditionally been separated from the wind-driven gyre circulation by assuming that the gyre flows horizontally along constant depth levels. By tracing the pathways of virtual water parcels in a high-resolution ocean model, we show that the heat transported by the subtropical gyre is larger than traditional estimates because water parcels spiral downwards across depth levels. Our results indicate that the subtropical gyre should not be considered separate from the overturning circulation, since the water parcels cooled within the gyre subsequently flow northwards to form cold, dense waters in the subpolar North Atlantic.

1. Introduction

Throughout the coming century, the Atlantic Meridional Overturning Circulation (AMOC) will play a critical role in shaping the response of the global climate system to anthropogenic activity through the redistribution of excess heat, freshwater and carbon. Since 2004, the Rapid Climate Change-Meridional Overturning Circulation and Heatflux Array (RAPID-MOCHA, herein referred to as RAPID) trans-basin observing system has made continuous measurements of the strength of the AMOC and the associated meridional transports of heat and freshwater across 26.5°N (Cunningham et al., 2007). Here, the subtropical North Atlantic Ocean transports approximately 1.2 PW of heat northwards (Hall & Bryden, 1982; Johns et al., 2011; McCarthy, Smeed, et al., 2015), accounting for 30% of the total ocean-atmosphere Meridional Heat Transport (MHT) (Ganachaud & Wunsch, 2000; Johns et al., 2023a; Trenberth & Fasullo, 2017).

Traditionally, the total ocean MHT across 26.5°N has been partitioned into zonally-averaged vertical and residual horizontal circulation components (Böning & Herrmann, 1994; Bryan, 1982; Johns et al., 2011), typically referred to as overturning and gyre heat transports, respectively. However, the degree to which these 2-dimensional geometric components represent the actual contributions made by the 3-dimensional flow structures of the AMOC and Subtropical Gyre (STG) to the total MHT at 26.5°N has been widely debated (e.g., Johns et al., 2023a; Talley, 2003). Previous studies have criticized this interpretation of the horizontal gyre circulation because the waters flowing northward within the western boundary current of the STG do not recirculate horizontally along constant depth surfaces, but rather spiral downwards to form Subtropical Mode Water (STMW) in a shallow local overturning cell (Berglund et al., 2022; Burkholder & Lozier, 2014; Spall, 1992; Talley, 2003). According to Talley (2003), this wind-driven STMW cell within the STG could account for up to 0.4 PW of the total MHT

Writing – review & editing: Oliver J. Tooth, Nicholas P. Foukal, William E. Johns, Helen L. Johnson, Chris Wilson

observed at 24°N, much larger than the traditionally defined horizontal gyre heat transport. In contrast, the modeling study of Xu et al. (2016) concludes that the STG makes a negligible contribution to the total MHT across 26.5°N since the authors argue that the near-surface waters of the Florida Current participate directly in the basin-scale AMOC rather than circulating around the STG.

The long-standing uncertainty regarding the relative contributions of the AMOC and the STG flow structures to the total MHT at 26.5°N ultimately reflects the subjective nature of approaching this problem within the confines of the traditional Eulerian framework (Johns et al., 2023a). To overcome this challenge, we present the first Lagrangian decomposition of the MHT and overturning across the RAPID 26.5°N array using water parcel trajectories evaluated within an eddy-rich ocean sea-ice hindcast simulation.

2. Materials and Methods

2.1. Ocean General Circulation Model

To investigate the meridional overturning and heat transport at 26.5°N, we use output from the ORCA0083-N06 ocean sea-ice hindcast simulation, documented in Moat et al. (2016). The simulation uses a global implementation of the Nucleus for European Modeling of the Ocean (NEMO) ocean circulation model version 3.6 (Madec, 2016) coupled to the Louvain-la-Neuve Ice Model version 2 (LIM2) sea-ice model (Bouillon et al., 2009). The ocean component is configured with a nominal horizontal resolution of 1/12° (equivalent to 8.3 km at 26.5°N) and with 75 unevenly spaced z-coordinate levels ranging from 1 to 250 m depth increments. The hindcast simulation is integrated for the historical period from 1958 to 2015 using the Drakkar Forcing Set 5.2 (Dussin et al., 2016). Here, we make use of the 5-day mean velocity and tracer fields output for the period 1980–2015.

Throughout this study, we compare the results derived from the ORCA0083-N06 simulation to observations made along the RAPID array at 26.5°N for the overlapping period 2004–2015 (Johns et al., 2023b). To ensure consistency between model and observational diagnostics, we implement a zero net volume transport constraint across 26.5°N, equivalent to that imposed by the RAPID program (e.g., Kanzow et al., 2010), in all Eulerian meridional overturning and heat transport calculations.

2.2. Lagrangian Particle Tracking

To determine the contributions of the STG and the basin-scale overturning circulation to the total MHT at 26.5°N, we calculate the Lagrangian trajectories of virtual water parcels advected by the time-evolving velocity fields of the ORCA0083-N06 hindcast using TRACMASS version 7.1 (Aldama-Campino et al., 2020).

To compare the results of our Lagrangian experiment with observations made along 26.5°N, we track water parcels flowing southward across the RAPID section backwards-in-time to determine their origin. In total, we initialize more than 12.3 million water parcels sampling the full-depth southward transport across 26.5°N over 144 months between 2004 and 2015. At the beginning of each month, the number of water parcels to be distributed evenly across each grid cell face (N_{gc}) is determined by:

$$N_{gc} = ceil\left(\frac{V_{gc}}{V_{\max}}\right) \quad (1)$$

where V_{gc} is the absolute southward transport and $V_{\max}$ represents a maximum volume transport of 0.005 Sv per parcel (1 Sv $\equiv 1 \times 10^6$ m^3 s^{-1}).

Water parcels are advected backwards-in-time using 5-day mean velocity fields for a maximum of 25 years to trace their origins. Water parcel trajectories are terminated on reaching this maximum advection time or when they meet any one of the following criteria (Figure 1a): (a) returning to the RAPID 26.5°N section, (b) reaching the Overturning in the Subpolar North Atlantic Program (OSNAP) array, or (c) reaching either the Gibraltar Strait (GS) or English Channel (EC). The overwhelming majority of trajectories initialized across 26.5°N also originate from 26.5°N (91.3%), indicating a robust recirculation of waters at this latitude. This large recirculating transport is dominated by short-lived trajectories capturing eddy recirculations in the ocean interior (197.3 ± 22.0 Sv), whereas only 20.6 ± 3.0 Sv is sourced directly from the Florida Current at 26.5°N. Importantly, Figure 1b shows

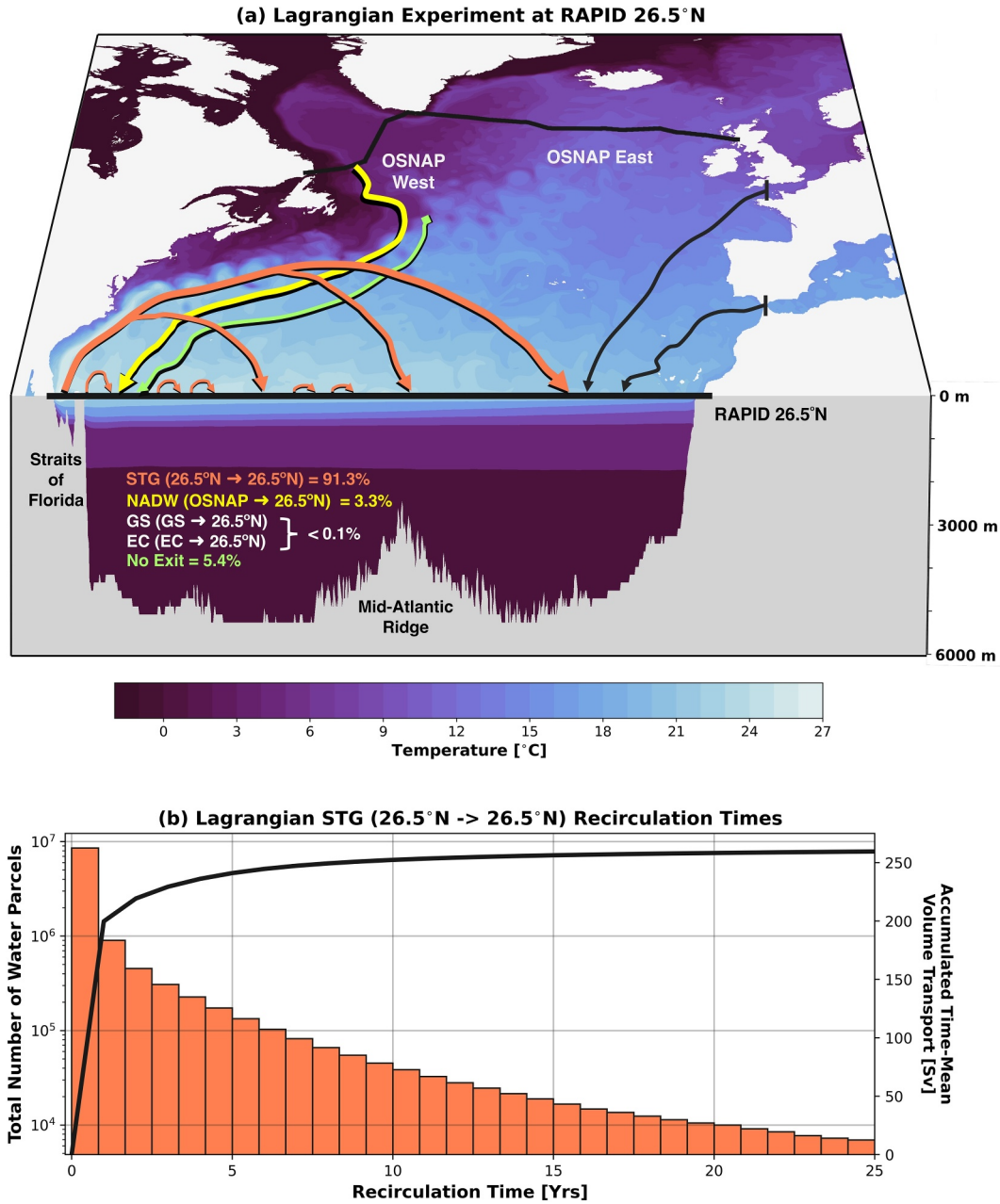

Figure 1. (a) Schematic representation of the Lagrangian pathways north of the RAPID array at 26.5°N. (b) Distribution of recirculation times for STG water parcels returning to 26.5°N within the 25-year maximum advection period. The solid black line overlaid shows the accumulation of the time-mean volume transport (Sv) of the STG pathway as a function of water parcel recirculation time.

that the 25-year maximum advection time is sufficient to fully resolve the STG circulation because the accumulated volume transport originating from 26.5°N has stabilized within this period.

We perform an additional Lagrangian experiment to determine the origins of the northward Florida Current transport by tracking trajectories backwards-in-time from the Florida Straits. We use the same water parcel initialization and advection strategy outlined above for consistency. In this experiment, we terminate water parcel trajectories on crossing one of two geographic boundaries (5°N or 26.5°N in Figure S1 in Supporting Information S1) or upon reaching the 25-year maximum advection time (<3%).

2.3. Diagnosing Meridional Overturning and Heat Transport at 26.5°N

We quantify the strength of the Eulerian overturning at 26.5°N by calculating meridional overturning streamfunctions in both depth (ψ_z) and density (ψ_{σ_θ}) coordinates:

$$\psi_z(z,t) = \int_z^0 \int_{x_w}^{x_e} v(x,\, z,\, t)\; dx\; dz \tag{2}$$

$$\psi_{\sigma_\theta}(\sigma_\theta,t) = \int_{x_w}^{x_e} \int_{z(x,\,\sigma_\theta,\,t)}^{0} v(x,\, z,\, t)\; dz\; dx, \tag{3}$$

where $v\,(x, z, t)$ is the meridional velocity and $z\,(x, \sigma_\theta, t)$ is the time-evolving depth of the isopycnal σ_θ across the trans-basin section between the eastern (x_e) and western (x_w) boundaries. We account for the time-evolving net volume transport across the section using a spatially uniform compensating meridional velocity (Kanzow et al., 2010).

The northward MHT across 26.5°N is calculated following Moat et al. (2016) by integrating the product of the meridional velocity $v\,(x, z, t)$ and potential temperature (θ) over the full depth $H(x)$:

$$Q_{Total}(t) = \int_{-H(x)}^{0} \int_{x_w}^{x_e} \rho_o c_p\; v(x,\, z,\, t)\; \theta(x,\, z,\, t)\; dx\; dz \tag{4}$$

where the product of the seawater density and the specific heat capacity of seawater is given by $\rho_o c_p = 4.1 \times 10^6$ J m^{-3} °C^{-1} following Johns et al. (2011). We further partition the total MHT across the RAPID section (Q_{Total}) into horizontal (Q_{horz}) and vertical (Q_{vert}) components (Bryden & Imawaki, 2001; Johns et al., 2011), as follows:

$$Q_{vert}(t) = \int_{-H}^{0} \int_{x_w}^{x_e} \rho_o c_p\; \langle v \rangle \langle \theta \rangle\; dx\; dz \tag{5}$$

$$Q_{horz}(t) = \int_{-H(x)}^{0} \int_{x_w}^{x_e} \rho_o c_p\; v^*(x,\, z,\, t)\; \theta^*(x,\, z,\, t)\; dx\; dz \tag{6}$$

where $\langle v \rangle$ and $\langle \theta \rangle$ represent the zonally averaged velocity and potential temperature profiles (both functions of depth), and v^* and θ^* represent deviations from these zonally averaged profiles.

To complement the Eulerian diagnostics outlined above, we additionally quantify the strength of overturning and MHT across 26.5°N from the Lagrangian water parcel trajectories initialized between 2004 and 2015. To determine the vertical and diapycnal overturning taking place within the STG, we calculate partial Lagrangian overturning streamfunctions (Blanke et al., 1999; Döös et al., 2008) using only the subset of $N(t)$ water parcels which return to 26.5°N within an advection period, τ, where $0 \le \tau \le 25$ years, as follows (Tooth et al., 2023):

$$F_z(z,\, t) = \sum_{z' = z_{\min}}^{z} \left(V_{North,z'}(t-\tau) - V_{South,z'}(t)\right) \tag{7}$$

$$F_{\sigma_\theta}(\sigma_\theta,\, t) = \sum_{\sigma_\theta' = \sigma_{\min}}^{\sigma_\theta} \left(V_{North,\sigma_\theta'}(t-\tau) - V_{South,\sigma_\theta'}(t)\right) \tag{8}$$

where V_{North} and V_{South} represent the absolute volume transport distributions of all recirculating STG water parcels on their northward and southward crossings of the RAPID 26.5°N section.

Since Döös et al. (2008) showed that, provided a sufficiently large number of water parcels are initialized, the total Lagrangian overturning streamfunction will converge toward the time-mean Eulerian streamfunction, it follows that the time-mean overturning of the NADW and AABW cells can be estimated by the residual $\overline{\psi_{\sigma_\theta}} - \overline{F_{\sigma_\theta}}$ (see

Text S2 in Supporting Information S1). Our Lagrangian decomposition uses the time-mean Eulerian overturning averaged over 2000–2015 because more than 90% of STG water parcels return to 26.5°N within 4 years of their initialization (Figure 1b).

We additionally define a Lagrangian measure of the MHT due to the $N(t)$ water parcels recirculating within the STG using their potential temperatures on their northward ($\theta_{North,i}$) and southward ($\theta_{South,i}$) crossings of the RAPID section at 26.5°N:

$$Q_{STG}(t) = \rho c_p \sum_{i \in N} V_i \left(\theta_{North,i}(t-\tau) - \theta_{South,i}(t)\right) \quad (9)$$

where V_i is the volume transport conveyed by an individual water parcel i returning to 26.5°N, which is conserved along its entire trajectory.

3. Evaluating Eulerian Meridional Overturning and Heat Transport at 26.5°N

We begin by adopting the traditional Eulerian frame of reference to compare the meridional overturning and heat transport simulated in ORCA0083-N06 to RAPID observations between 2004 and 2015. Although there is strong agreement between the modeled and observed time-mean vertical overturning streamfunctions at 26.5°N (see Figure S2 in Supporting Information S1), we find that the simulated vertical overturning strength (15.1 ± 2.8 Sv) is around 2 Sv weaker than observed (17.0 ± 3.6 Sv).

Figures 2a and 2b present equivalent decompositions of the Eulerian heat transport across 26.5°N in both RAPID observations and the ORCA0083-N06 hindcast. Concordant with its weaker than observed overturning, the model time-mean MHT is 0.98 ± 0.21 PW compared with 1.2 ± 0.28 PW in observations. The model does, however, reproduce many features of the overturning and heat transport variability recorded in observations (Moat et al., 2016), including the reduction in overturning between 2009 and 2010 (McCarthy et al., 2012). Observations show that both the magnitude and variability of the MHT at 26.5°N is dominated (>90%) by the vertical component, while <10% is associated with the horizontal circulation (Johns et al., 2011; Johns et al., 2023a; McCarthy, Haigh, et al., 2015). Figure 2b shows a similar vertical-horizontal partition in ORCA0083-N06; the vertical cell accounts for 85% (0.84 ± 0.21 PW), and the horizontal cell for the remaining 15% (0.14 ± 0.06 PW) of the total MHT.

A closer examination of the simulated hydrography along 26.5°N shows that both the volume transport (31.3 ± 1.8 Sv) and temperature transport (2.56 ± 0.14 PW) of the Florida Current are well represented in the model compared with observed estimates reported in Meinen et al. (2010) and Johns et al. (2023a). Moat et al. (2016) highlighted the larger than observed southward Mid-Ocean (WB2 mooring to Africa) heat transport component in ORCA0083-N06 as a likely source of the model's underestimation of the observed total MHT. Figure 2c shows that, in the model, more of the warm and shallow waters transported northwards in the Florida Current are returned in the upper 100 m of the Mid-Ocean region along the RAPID array compared with observations. This is in contrast to previous studies, which have attributed the widespread underestimation of subtropical MHT in numerical models (e.g., Liu et al., 2022) to the overly diffusive thermocline simulated in z-coordinates (Msadek et al., 2013; Roberts et al., 2020), which results in a warmer than observed AMOC lower limb. Notably, there is good agreement between the basin-wide average potential temperature profiles simulated in ORCA0083-N06 and observed along the RAPID array (Figure 2d), with even a slightly sharper main thermocline (between depths of 400–800 m) in the model than in observations.

Since we propose that the excess shallow return flow in the STG accounts for the model's underestimation of MHT compared with RAPID observations, we next consider how this bias might influence the relative contribution of the STG circulation to total MHT across 26.5°N. By examining the Lagrangian trajectories sourced from the upper Florida Current, we determine that rapidly recirculated water parcels return southward in the upper 100 m of the Mid-Ocean region between 75.5°W and 72°W (Figure 3a) where potential temperatures typically exceed 23°C. We will later show that STG water parcels flowing southward across 26.5°N in this potential temperature range contribute negligibly to the time-mean MHT when averaged on longer than seasonal timescales (see Figure 3d). As such, we do not expect the underestimation of MHT in ORCA0083-N06 to impact the relative heat transport contributions of the STG and the basin-scale overturning circulations identified in this study.

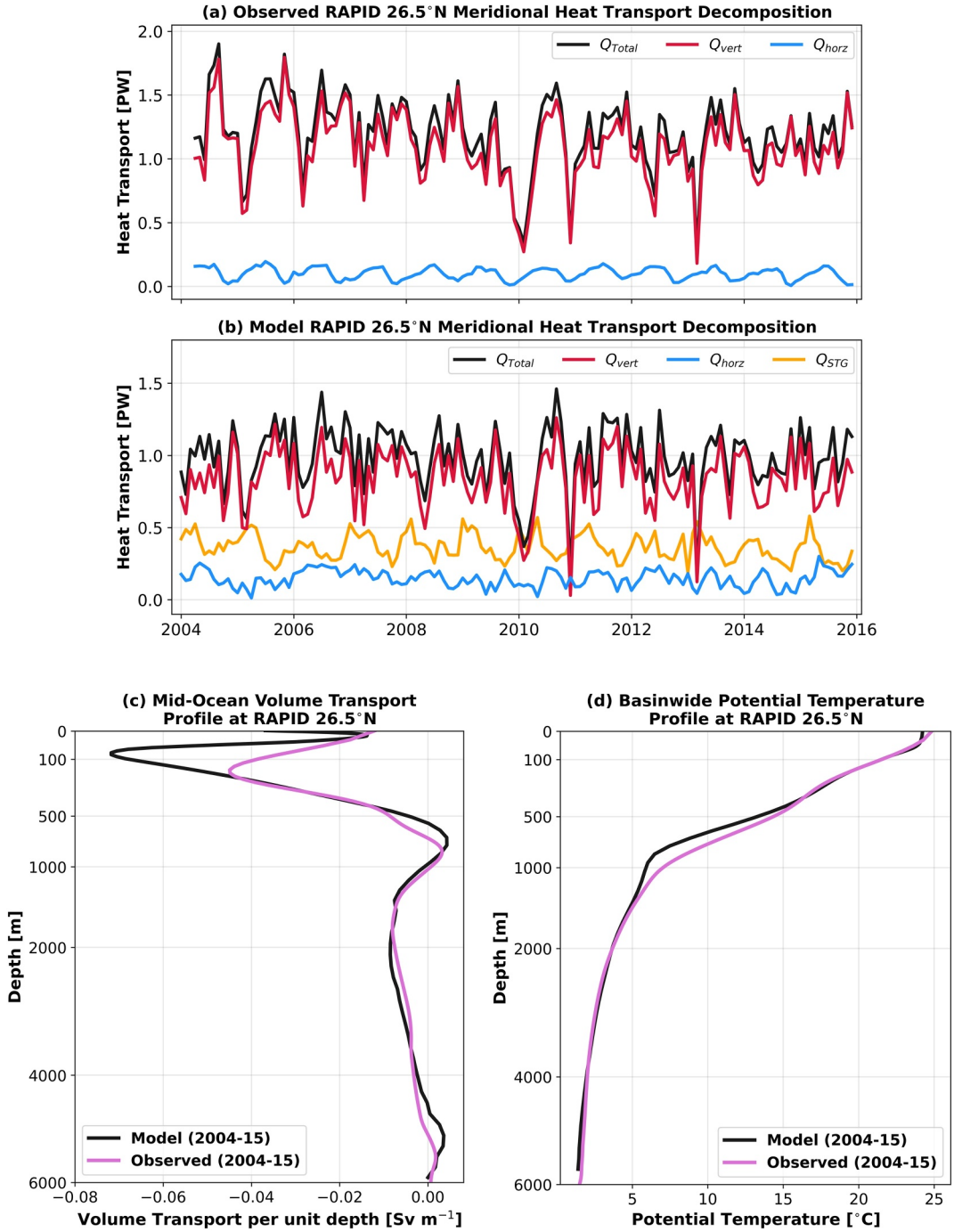

Figure 2. (a) Total observed MHT (black) at 26.5°N decomposed into a zonally-averaged vertical cell (Q_{vert}, red) and a residual horizontal cell (Q_{horz}, blue). (b) As in (a) but calculated using model Eulerian meridional velocity and potential temperature fields at 26.5°N. The STG heat transport calculated using recirculating trajectories (Q_{STG}, orange) is plotted according to the month water parcels flow southward across 26.5°N. (c) Model (black) and observed (pink) time-mean (2004–2015) meridional volume transport per unit depth (Sv m^{-1}) in the Mid-Ocean region (Bahamas to Africa). (d) Time-mean (2004–2015) potential temperature profiles (°C) for the entire basin (Straits of Florida to Africa) in the model (black) and RAPID observations (pink). Note that we use non-linear vertical axes in (c) and (d) to highlight the upper 500 m.

Overall, we find sufficient agreement between the structure and variability of both the vertical overturning and MHT simulated by ORCA0083-N06 and observations to justify our use of the model to better understand the contributions made by the STG and basin-scale overturning circulation to the MHT at RAPID 26.5°N.

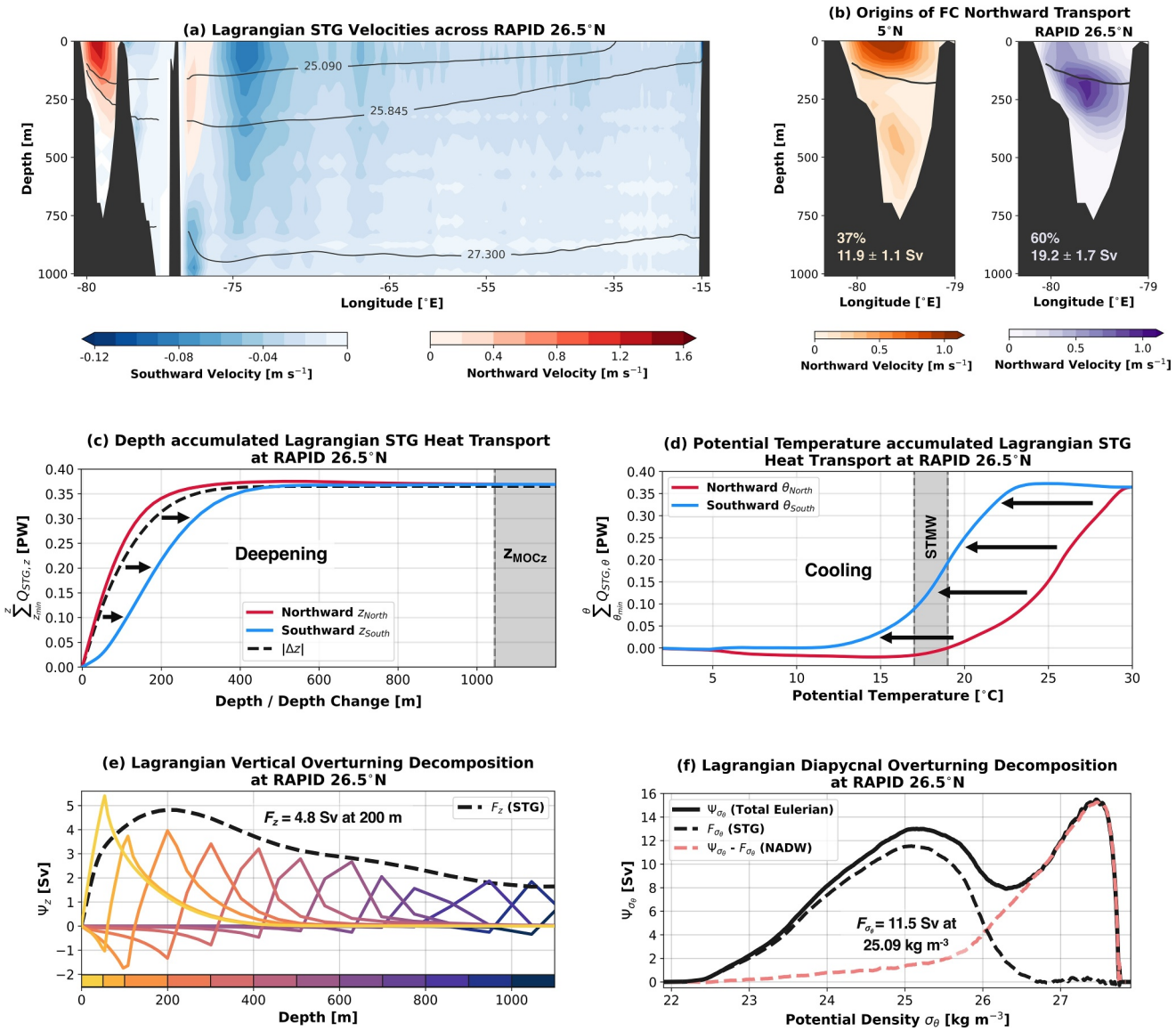

Figure 3. (a) Distribution of STG water parcel northward (red contours) and southward (blue contours) crossings of the RAPID 26.5°N section shown as an effective velocity (m s^{-1}). Note that the longitude axis is stretched to highlight the Florida Current. (b) Origins of the Florida Current (FC) northward transport shown as the effective velocity (m s^{-1}) of waters sourced from the tropical North Atlantic (5°N) and the STG recirculation (RAPID 26.5°N). The $\sigma_\theta = 25.09$ kg m^{-3} time-mean isopycnal surface is overlaid. Heat transport of the STG circulation accumulated as a function of the (c) absolute depth change (black dashed), depth and (d) potential temperature of recirculating water parcels between/on their northward (red) and southward (blue) crossings of 26.5°N. The depth of maximum Eulerian overturning in depth-space, $z_{MOC} = 1045$ m is indicated by the gray dashed line in (c). The shaded region in (d) defines STMW (17–19°C) following Kwon and Riser (2004). (e) Time-mean (2004–2015) vertical overturning streamfunction of the STG circulation (F_z, black dashed) decomposed according to the depth of water parcels on their northward crossing of 26.5°N. Water parcels are grouped into discrete depth layers defined in the lower colorbar. (f) Lagrangian decomposition of the time-mean (2004–2015) diapycnal overturning streamfunction at 26.5°N (ψ_{σ_θ}, black solid) into a STG component (F_{σ_θ}, black dashed), determined from recirculating water parcels, and a residual NADW component (ψ_{σ_θ} - F_{σ_θ}, pink dashed).

4. Lagrangian Decomposition of Meridional Overturning and Heat Transport at 26.5°N

To complement the traditional Eulerian vertical-horizontal decomposition, we use our Lagrangian trajectories to quantify the contribution made by water parcels which recirculate in the STG to the time-mean MHT at 26.5°N. We find that the STG circulation accounts for 0.36 ± 0.09 PW or 37 ± 9% of the total MHT across 26.5°N in the model (Figure 2b). This implies that the heat transport of the STG is more than twice that of the horizontal gyre heat transport component (0.14 ± 0.06 PW) and is in closer agreement with the observed estimate of 0.4 PW at

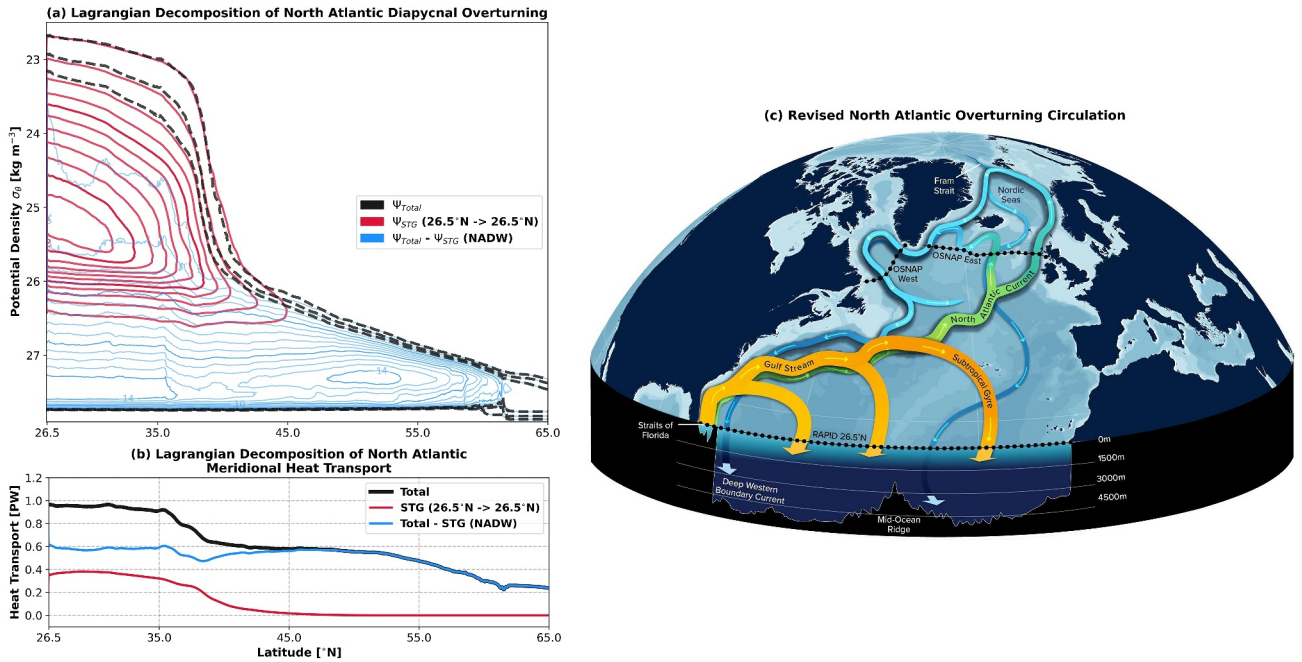

Figure 4. (a) Lagrangian decomposition of the time-mean (2000–2015) North Atlantic Ocean diapycnal overturning streamfunction north of RAPID 26.5°N into a STG component (red), derived from recirculating water parcel trajectories, and a residual component (NADW cell, blue). Selected streamlines (1, 2, 3 Sv) of the total Eulerian overturning streamfunction are overlaid in black (dashed). (b) Lagrangian decomposition of the latitudinal distribution of the time-mean North Atlantic Ocean MHT (black) into the contributions of the STG cell (red) and residual NADW cell (blue). (c) Schematic depicting the principal circulation components of the Atlantic Meridional Overturning Circulation (AMOC) north of the RAPID 26.5°N section.

24°N (Talley, 2003). Figure 3a additionally confirms the assumption of Talley (2003) that the lightest waters flowing northward in the upper Florida Current ($\sigma_\theta < 25.875$) are returned across 26.5°N via the broad southward interior flow ($\sigma_\theta < 27.3$) between the Bahamas and Africa. In total, we find that 72% of STG heat transport is sourced from water parcels flowing northward in the upper 150 m of the Florida Current, which overwhelmingly originate from the tropical North Atlantic (5°N in Figure 3b). Further, Figure 3b clearly shows that the thermocline waters flowing northward in the Florida Current are predominantly sourced from the STG along 26.5°N.

We find that STG heat transport is dominated by water parcels which participate in a shallow vertical overturning cell north of 26.5°N (Figure 3c). More specifically, Figures 3c and 3d show that the entire MHT of the STG can be explained by trajectories which follow a downwards cooling spiral within the upper 500 m of the AMOC upper limb ($z_{MOC} = 1045$ m). Interestingly, although STG heat transport depends strongly on along-stream diapycnal (diathermal) transformation, STMW formation can only account for 29% of the total MHT of the STG (17°C $\leq \theta_{South} \leq$ 19°C in Figure 3d). Diapycnal transformation within the STG instead peaks at lighter density classes ($\theta \approx 22.7$°C or $\sigma_\theta = 25.09$ kg m^{-3} in Figure 3f), including Subtropical Underwater (STUW; O'Connor et al., 2005), which accounts for 47% of the STG heat transport ($\theta_{South} > 19$°C in Figure 3d).

A particularly surprising finding is the large 6.7 Sv discrepancy between the strength of vertical (4.8 Sv in Figure 3e) and diapycnal (11.5 Sv in Figure 3f) overturning in the STG. Previous studies in the subpolar North Atlantic have interpreted the similar discrepancy there as evidence for a substantial horizontal circulation across sloping isopycnals (Zhang & Thomas, 2021). However, Figure 3e reveals that here in the subtropical North Atlantic, this discrepancy is, in fact, due to the underestimation of STG vertical overturning, which results from compensation between the northward and southward flowing limbs of the downward spiral when accumulated along constant depth levels. This is analogous to that of the Deacon cell in the Southern Ocean (Döös & Webb, 1994) and illustrates how the downward spiraling behavior of the STG circulation (Berglund et al., 2022) is concealed by the superposition of many shallow overturning cells in the vertical overturning streamfunction (Figure 3e; Döös et al., 2008).

By subtracting the diapycnal overturning associated with STG water parcels from the time-mean Eulerian overturning streamfunctions in Figures 3f and 4a, we obtain an estimate for the contribution of the NADW cell to

the total overturning in density-space at 26.5°N. The residual diapycnal overturning streamfunctions, in combination with Figure 3b (RAPID 26.5°N) and Figure S3 in Supporting Information S1, confirm the earlier propositions of Burkholder and Lozier (2014) and Qu et al. (2013) that the mode waters returned in the southward limb of the shallow STG overturning cell are the principal source waters for the northward, subsurface limb of the NADW cell. Meanwhile, the remainder of the NADW cell is sourced directly from denser waters ($\sigma_\theta > 26.5$ kg m^{-3}) originating in the tropical North Atlantic, which flow northward across 26.5°N at depth in the Florida Current (Figure 3b and Figure S3 in Supporting Information S1).

5. Discussion and Conclusions

In this study, we present the first Lagrangian decomposition of the meridional overturning and heat transport at 26.5°N using an eddy-rich ocean hindcast. We show that water parcels circulating around the STG account for 37% (0.36 PW) of the total MHT across 26.5°N, more than twice that of the classical horizontal gyre component (15%). This underestimation of STG heat transport is attributable to the downward spiraling nature of the STG recirculation (Berglund et al., 2022; Spall, 1992), which imprints onto a shallow vertical overturning cell rather than the horizontal circulation across 26.5°N.

Our Lagrangian analysis demonstrates that the MHT of the STG overturning cell is analogous to a subtropical mode water cascade (Blanke et al., 2002) in which water parcels arriving in the upper Florida Current are successively transformed toward intermediate densities via a downwards cooling spiral (Spall, 1992). The spiral begins with the convective formation and lateral subduction of STUW varieties (O'Connor et al., 2005; Qu et al., 2016), which account for 47% of STG heat transport. The subsequent transformation of recirculating STUW into STMW via intense wintertime cooling along the path of the Gulf Stream (e.g., Joyce et al., 2013) surprisingly explains less than a third of STG heat transport. The downwards cooling spiral, which typically spans several decades (Berglund et al., 2022), concludes when STG water parcels reach the required depth ($z > 200$ m) and density ($\sigma_\theta > 25.5$ kg m^{-3}) to be exported northward in the subsurface limb of the large-scale NADW cell (Figure 3f and Figure S3 in Supporting Information S1).

In contrast to the STG overturning cell, the NADW cell spans both subtropical and subpolar latitudes (Figure 4a), because the weaker potential vorticity gradient across the Gulf Stream at depth permits water parcels to be advected north-eastward via the subsurface pathways of the North Atlantic Current (Bower & Lozier, 1994; Burkholder & Lozier, 2011; Gary et al., 2014; Jacobs et al., 2019). This northward subsurface branch of the NADW cell was arguably first identified as a 'nutrient stream' from the biogeochemical observations of Pelegrí and Csanady (1991). The nutrient stream plays a fundamental role in maintaining biological productivity at high latitudes by transporting large concentrations of nutrients along shoaling isopycnals which outcrop within the eastern subpolar gyre (SPG) (Williams et al., 2011). There are two important implications of this subsurface subtropical to surface subpolar connectivity (Burkholder & Lozier, 2014). Firstly, water parcels flowing northward in the NADW cell experience negligible heat loss prior to reaching the southern limit of the SPG (~47°N in Figure 4b) and hence the heat transport divergence between 26.5°N and the inter-gyre boundary is equivalent to the STG heat transport (0.36 PW). Secondly, no inter-gyre pathway exists for sea surface temperature anomalies originating in the Gulf Stream to propagate advectively toward the eastern SPG (Foukal & Lozier, 2016). This highlights the central challenge of inferring large-scale circulation from Eulerian overturning stream functions since the streamlines presented in Figure 4a misleadingly suggest a continuous meridional pathway from the lightest to the densest water masses in the North Atlantic while, in fact, there are two overlapping diapycnal cells, which are, themselves, the superposition of many smaller overturning cells.

Although the strength of our conclusions is limited by the use of a single eddy-rich ocean hindcast, we note the strong agreement between our findings and those of Ferrari and Ferreira (2011), who used model sensitivity experiments to suggest that 40% of North Atlantic MHT is associated with the wind-driven STG circulation, whereas the remaining 60% is due to high latitude convection. Moreover, when our estimate of STG heat transport (37%) is applied to observations along 26.5°N, this translates to 0.44 PW of the total 1.2 PW due to the STG circulation, which is in close agreement with the 0.42 PW (35%) estimated by Johns et al. (2023a) when applying the approach of Talley (2003) to RAPID observations. The remaining 0.76 PW (63%) of the total observed MHT across 26.5°N is due to the formation of NADW within the SPG and the Nordic Seas. These two regions exhibit complex overturning geometries, with a substantial fraction of dense water formation owed to horizontal circulation across sloping isopycnals (Hirschi et al., 2020; Xu et al., 2018; Zhang & Thomas, 2021).

In contrast to the traditional conveyor-belt view of North Atlantic overturning, our Lagrangian analysis demonstrates that both vertical and horizontal circulation cells are fundamental components of the AMOC and thus basin-scale overturning cannot be meaningfully distinguished from the gyre circulations of the North Atlantic (Figure 4c). A more natural decomposition of the AMOC is between the STG and NADW diapycnal overturning cells shown in Figure 4a since these capture the successive transformations required to form dense NADW from the lightest waters flowing northward in the Florida Current. Extending the Lagrangian analysis presented here to reveal the phenomenology of overturning variability within each of these circulation cells and their interconnectivity across timescales is the subject of future research.

Data Availability Statement

The Lagrangian trajectory crossings of the RAPID 26.5°N section used in our analysis can be obtained from Tooth (2023). The Lagrangian trajectory code TRACMASS was developed by Aldama-Campino et al. (2020). Data from the RAPID-MOCHA program are funded by the U.S. National Science Foundation and U.K. Natural Environment Research Council and are freely available to the public at https://www.rapid.ac.uk/rapidmoc and https://mocha.rsmas.miami.edu/mocha. The specific version of the observed RAPID-MOCHA heat transport data used in this study is Johns et al. (2023b).

Acknowledgments

O.J. Tooth is grateful for the financial support of the UK Natural Environment Research Council (NE/S007474/1). N.P. Foukal was supported by the Andrew W. Mellon Foundation Endowed Fund for Innovative Research from the Woods Hole Oceanographic Institution and Grant OCE-2047952 from the U. S. National Science Foundation. W.E. Johns was supported by the Grants OCE-1926008 and OCE-2148723 from the U.S. National Science Foundation. H.L. Johnson was supported by the NERC-NSF Grant SNAP-DRAGON (NE/T013494/1). C.W. was jointly supported by the NERC LTS-S CLASS (Climate-Linked Atlantic Sector Science) Grant (NE/R015953/1) and the NERC LTS-M CANARI (Climate change in the Arctic-North Atlantic Region and Impacts on the UK) Grant (NE/W004984/1). We are grateful to the WHOI Creative Studio for the production of Figure 4c.

References

Aldama-Campino, A., Döös, K., Kjellsson, J., & Jönsson, B. (2020). TRACMASS: Formal release of version 7.0 (v7.0-beta). [Software]. *Zenodo*. https://doi.org/10.5281/zenodo.4337926

Berglund, S., Döös, K., Groeskamp, S., & McDougall, T. J. (2022). The downward spiralling nature of the North Atlantic Subtropical Gyre. *Nature Communications*, *13*(1), 2000. https://doi.org/10.1038/s41467-022-29607-8

Blanke, B., Arhan, M., Lazar, A., & Prévost, G. (2002). A Lagrangian numerical investigation of the origins and fates of the salinity maximum water in the Atlantic. *Journal of Geophysical Research*, *107*(C10). https://doi.org/10.1029/2002JC001318

Blanke, B., Arhan, M., Madec, G., & Roche, S. (1999). Warm water paths in the equatorial Atlantic as diagnosed with a General Circulation Model. *Journal of Physical Oceanography*, *29*(11), 2753–2768. https://doi.org/10.1175/1520-0485(1999)029⟨2753:WWPITE⟩2.0.CO;2

Böning, C. W., & Herrmann, P. (1994). Annual cycle of poleward heat transport in the Ocean: Results from high-resolution modeling of the North and Equatorial Atlantic. *Journal of Physical Oceanography*, *24*(1), 91–107. https://doi.org/10.1175/1520-0485(1994)024⟨0091:ACOPHT⟩2.0.CO;2

Bouillon, S., Ángel Morales Maqueda, M., Legat, V., & Fichefet, T. (2009). An elastic–viscous–plastic sea ice model formulated on arakawa b and c grids. *Ocean Modelling*, *27*(3), 174–184. https://doi.org/10.1016/j.ocemod.2009.01.004

Bower, A., & Lozier, M. (1994). A closer look at particle exchange in the Gulf stream. *Journal of Physical Oceanography*, *24*(6), 1399–1418. https://doi.org/10.1175/1520-0485(1994)024<1399:aclape>2.0.co;2

Bryan, K. (1982). Seasonal variation in meridional overturning and poleward heat transport in the Atlantic and Pacific oceans: A model study. *Journal of Marine Research*, *40*, 39–53.

Bryden, H., & Imawaki, S. (2001). Ocean heat transport [Book section]. In G. Siedler, J. Church, & J. Gould (Eds.), *Ocean circulation and climate: Observing and modelling the global ocean*, *International Geophysics Series No. 77* (pp. 455–474). Academic Press.

Burkholder, K. C., & Lozier, M. S. (2011). Subtropical to subpolar pathways in the North Atlantic: Deductions from Lagrangian trajectories. *Journal of Geophysical Research*, *116*(C7). https://doi.org/10.1029/2010JC006697

Burkholder, K. C., & Lozier, M. S. (2014). Tracing the pathways of the upper limb of the north atlantic meridional overturning circulation. *Geophysical Research Letters*, *41*(12), 4254–4260. https://doi.org/10.1002/2014GL060226

Cunningham, S., Kanzow, T., Rayner, D., Baringer, M., Johns, W., Marotzke, J., et al. (2007). Temporal variability of the Atlantic meridional overturning circulation at 26.5°N. *Science*, *317*(5840), 935–938. https://doi.org/10.1126/science.1141304

Döös, K., Nycander, J., & Coward, A. C. (2008). Lagrangian decomposition of the deacon cell. *Journal of Geophysical Research*, *113*(C7). https://doi.org/10.1029/2007JC004351

Döös, K., & Webb, D. J. (1994). The deacon cell and the other meridional cells of the southern ocean. *Journal of Physical Oceanography*, *24*(2), 429–442. https://doi.org/10.1175/1520-0485(1994)024⟨0429:TDCATO⟩2.0.CO;2

Dussin, R., Barnier, B., Brodeau, L., & Molines, J. M. (2016). The making of the DRAKKAR forcing set DFS5 (Technical report). Retrieved from https://www.drakkar-ocean.eu/publications/reports/report/DFS5v3/April2016.pdf

Ferrari, R., & Ferreira, D. (2011). What processes drive the ocean heat transport? *Ocean Modelling*, *38*(3–4), 171–186. https://doi.org/10.1016/j.ocemod.2011.02.013

Foukal, N., & Lozier, M. (2016). No inter-gyre pathway for sea-surface temperature anomalies in the north atlantic. *Nature Communications*, *7*(1), 11333. https://doi.org/10.1038/ncomms11333

Ganachaud, A., & Wunsch, C. (2000). Improved estimates of global ocean circulation, heat transport and mixing from hydrographic data. *Nature*, *408*(6811), 453–457. https://doi.org/10.1038/35044048

Gary, S., Lozier, M., Kwon, Y., & Park, J. (2014). The fate of north Atlantic subtropical mode water in the flame model. *Journal of Physical Oceanography*, *44*(5), 1354–1371. https://doi.org/10.1175/JPO-D-13-0202.1

Hall, M., & Bryden, H. (1982). Direct estimates and mechanisms of ocean heat transport. *Deep-Sea Research*, *29*(29), 339–359. https://doi.org/10.1016/0198-0149(82)90099-1

Hirschi, J. J.-M., Barnier, B., Böning, C., Biastoch, A., Blaker, A. T., Coward, A., et al. (2020). The atlantic meridional overturning circulation in high-resolution models. *Journal of Geophysical Research: Oceans*, *125*(4), e2019JC015522. https://doi.org/10.1029/2019JC015522

Jacobs, Z. L., Grist, J. P., Marsh, R., & Josey, S. A. (2019). A subannual subsurface pathway from the Gulf Stream to the subpolar Gyre and its role in warming and salinification in the 1990s. *Geophysical Research Letters*, *46*(13), 7518–7526. https://doi.org/10.1029/2019GL083021

Johns, W., Baringer, M., Beal, L., Cunningham, S., Kanzow, T., Bryden, H., et al. (2011). Continuous, array-based estimates of Atlantic Ocean heat transport at 26.5°N. *Journal of Climate*, *24*(10), 2429–2449. (Place: Boston MA, USA Publisher: American Meteorological Society). https://doi.org/10.1175/2010JCLI3997.1

Johns, W., Elipot, S., Smeed, D., Moat, B., King, B., Volkov, D., & Smith, R. (2023a). Towards two decades of Atlantic Ocean mass and heat transports at 26.5°N. *Philosophical Transactions of the Royal Society A: Mathematical, Physical & Engineering Sciences*, *381*(2262), 20220188. https://doi.org/10.1098/rsta.2022.0188

Johns, W., Elipot, S., Smeed, D., Moat, B., King, B., Volkov, D., & Smith, R. (2023b). (v.2020) Atlantic meridional overturning circulation (AMOC) heat transport time series between April 2004 and December 2020 at 26.5°N. [Dataset]. *University of Miami Libraries*. https://doi.org/10.17604/3nfq-va20

Joyce, T. M., Thomas, L. N., Dewar, W. K., & Girton, J. B. (2013). Eighteen degree water formation within the gulf stream during climode. *Deep Sea Research Part II: Topical Studies in Oceanography*, *91*, 1–10. https://doi.org/10.1016/j.dsr2.2013.02.019

Kanzow, T., Cunningham, S. A., Johns, W. E., Hirschi, J. J.-M., Marotzke, J., Baringer, M. O., et al. (2010). Seasonal variability of the Atlantic meridional overturning circulation at 26.5°N. *Journal of Climate*, *23*(21), 5678–5698. https://doi.org/10.1175/2010JCLI3389.1

Kwon, Y., & Riser, S. (2004). North Atlantic subtropical mode water: A history of ocean-atmosphere interaction 1961–2000. *Geophysical Research Letters*, *31*(19). https://doi.org/10.1029/2004GL021116

Liu, C., Yang, Y., Liao, X., Cao, N., Liu, J., Ou, N., et al. (2022). Discrepancies in simulated ocean net surface heat fluxes over the North Atlantic. *Advances in Atmospheric Sciences*, *39*(11), 1941–1955. https://doi.org/10.1007/s00376-022-1360-7

Madec, G. (2016). NEMO ocean engine. In *Note du Pôle Modélisation de l'Institut Pierre-Simon Laplace 27 (Technical Report)*. Retrieved from https://zenodo.org/records/3248739

McCarthy, G., Frajka-Williams, E., Johns, W., Baringer, M., Meinen, C., Bryden, H., et al. (2012). Observed interannual variability of the Atlantic meridional overturning circulation at 26.5°N. *Geophysical Research Letters*, *39*(19). https://doi.org/10.1029/2012GL052933

McCarthy, G., Haigh, I., Hirschi, J., Grist, J., & Smeed, D. (2015). Ocean impact on decadal Atlantic climate variability revealed by sea-level observations. *Nature*, *521*(7553), 508–510. https://doi.org/10.1038/nature14491

McCarthy, G., Smeed, D., Johns, W., Frajka-Williams, E., Moat, B., Rayner, D., et al. (2015). Measuring the Atlantic meridional overturning circulation at 26°N. *Progress in Oceanography*, *130*, 91–111. https://doi.org/10.1016/j.pocean.2014.10.006

Meinen, C. S., Baringer, M. O., & Garcia, R. F. (2010). Florida Current transport variability: An analysis of annual and longer-period signals. *Deep Sea Research Part I: Oceanographic Research Papers*, *57*(7), 835–846. https://doi.org/10.1016/j.dsr.2010.04.001

Moat, B. I., Josey, S. A., Sinha, B., Blaker, A. T., Smeed, D. A., McCarthy, G. D., et al. (2016). Major variations in subtropical North Atlantic heat transport at short (5 day) timescales and their causes. *Journal of Geophysical Research: Oceans*, *121*(5), 3237–3249. https://doi.org/10.1002/2016JC011660

Msadek, R., Johns, W. E., Yeager, S. G., Danabasoglu, G., Delworth, T. L., & Rosati, A. (2013). The Atlantic meridional heat transport at 26.5°N and its relationship with the MOC in the RAPID array and the GFDL and NCAR coupled models. *Journal of Climate*, *26*(12), 4335–4356. https://doi.org/10.1175/JCLI-D-12-00081.1

O'Connor, B. M., Fine, R. A., & Olson, D. B. (2005). A global comparison of subtropical underwater formation rates. *Deep Sea Research Part I: Oceanographic Research Papers*, *52*(9), 1569–1590. https://doi.org/10.1016/j.dsr.2005.01.011

Pelegrí, J. L., & Csanady, G. T. (1991). Nutrient transport and mixing in the Gulf Stream. *Journal of Geophysical Research*, *96*(C2), 2577–2583. https://doi.org/10.1029/90JC02535

Qu, T., Gao, S., & Fukumori, I. (2013). Formation of salinity maximum water and its contribution to the overturning circulation in the north Atlantic as revealed by a global general circulation model. *Journal of Geophysical Research: Oceans*, *118*(4), 1982–1994. https://doi.org/10.1002/jgrc.20152

Qu, T., Zhang, L., & Schneider, N. (2016). North Atlantic subtropical underwater and its year-to-year variability in annual subduction rate during the Argo period. *Journal of Physical Oceanography*, *46*(6), 1901–1916. https://doi.org/10.1175/JPO-D-15-0246.1

Roberts, M. J., Jackson, L. C., Roberts, C. D., Meccia, V., Docquier, D., Koenigk, T., et al. (2020). Sensitivity of the atlantic meridional overturning circulation to model resolution in CMIP6 HighResMIP simulations and implications for future changes. *Journal of Advances in Modeling Earth Systems*, *12*(8), e2019MS002014. https://doi.org/10.1029/2019MS002014

Spall, M. A. (1992). Cooling spirals and recirculation in the subtropical Gyre. *Journal of Physical Oceanography*, *22*(5), 564–571. https://doi.org/10.1175/1520-0485(1992)022⟨0564:CSARIT⟩2.0.CO;2

Talley, L. D. (2003). Shallow, intermediate, and deep overturning components of the global heat budget. *Journal of Physical Oceanography*, *33*(3), 530–560. https://doi.org/10.1175/1520-0485(2003)033⟨0530:SIADOC⟩2.0.CO;2

Tooth, O. (2023). Lagrangian decomposition of the meridional heat transport at 26.5N - Water parcel crossings of the rapid 26.5N array. [Dataset]. *Zenodo*. https://doi.org/10.5281/zenodo.10069800

Tooth, O., Johnson, H., Wilson, C., & Evans, D. (2023). Seasonal overturning variability in the eastern North Atlantic subpolar gyre: A Lagrangian perspective. *Ocean Science*, *19*(3), 769–791. https://doi.org/10.5194/os-19-769-2023

Trenberth, K. E., & Fasullo, J. T. (2017). Atlantic meridional heat transports computed from balancing Earth's energy locally. *Geophysical Research Letters*, *44*(4), 1919–1927. https://doi.org/10.1002/2016GL072475

Williams, R. G., McDonagh, E., Roussenov, V. M., Torres-Valdes, S., King, B., Sanders, R., & Hansell, D. A. (2011). Nutrient streams in the North Atlantic: Advective pathways of inorganic and dissolved organic nutrients. *Global Biogeochemical Cycles*, *25*(4). https://doi.org/10.1029/2010GB003853

Xu, X., Rhines, P. B., & Chassignet, E. P. (2016). Temperature–Salinity structure of the North Atlantic circulation and associated heat and freshwater transports. *Journal of Climate*, *29*(21), 7723–7742. https://doi.org/10.1175/JCLI-D-15-0798.1

Xu, X., Rhines, P. B., & Chassignet, E. P. (2018). On mapping the diapycnal water mass transformation of the upper North Atlantic Ocean. *Journal of Physical Oceanography*, *48*(10), 2233–2258. https://doi.org/10.1175/JPO-D-17-0223.1

Zhang, R., & Thomas, M. (2021). Horizontal circulation across density surfaces contributes substantially to the long-term mean northern Atlantic Meridional Overturning Circulation. *Communications Earth & Environment*, *2*(1), 112. https://doi.org/10.1038/s43247-021-00182-y

References From the Supporting Information

Döös, K., Jönsson, B., & Kjellsson, J. (2017). Evaluation of oceanic and atmospheric trajectory schemes in the TRACMASS trajectory model v6.0. *Geoscientific Model Development*, *10*(4), 1733–1749. https://doi.org/10.5194/gmd-10-1733-2017

McDougall, T. J., Jackett, D. R., Millero, F. J., Pawlowicz, R., & Barker, P. M. (2012). A global algorithm for estimating Absolute Salinity. *Ocean Science*, *8*(6), 1123–1134. https://doi.org/10.5194/os-8-1123-2012